Quantum measurement of dynamic qubit information by a double quantum-dot detector



2008 J. Phys.: Condens. Matter 20 075210

(http://iopscience.iop.org/0953-8984/20/7/075210)

J. Phys.: Condens. Matter **20** (2008) 075210 (6pp) doi:10.1088/0953-8984/20/7/075210

# Quantum measurement of dynamic qubit information by a double quantum-dot detector

**Zhao-Tan Jiang[1], J Yang[1] and Q Z Han[2,3]**

[1] Department of Physics, Beijing Institute of Technology, Beijing 100081, People's Republic of China
[2] Multi-Phase Reaction Laboratory, Institute of Process Engineering, Chinese Academy of Sciences, PO Box 353, Beijing 100080, People's Republic of China
[3] Graduate School of Chinese Academy of Sciences, PO Box 4588, Beijing 100049, People's Republic of China

E-mail: jiangzhaotan@bit.edu.cn

Received 5 September 2007, in final form 22 November 2007
Published 28 January 2008
Online at stacks.iop.org/JPhysCM/20/075210

**Abstract**

In this paper we propose a novel measurement scheme, based on a double quantum-dot detector, for reading out the qubit information sensed by the detector as a variation of the interdot coupling. By investigating the detector in the static qubit case, we find a sensitive qubit–detector response region determined by the detector geometry. Then we study quantum measurement of the information stored in a dynamic qubit. It is verified that whether the detector can perform well is closely dependent on the ratio of the right dot–lead coupling to interdot coupling in the detector, while the interdot Coulomb interaction only plays a trivial role. Furthermore, it is shown that the dephasing time of the qubit is strongly influenced by the difference between the interdot couplings of the detector corresponding to two qubit states. This work provides some helpful instructions on how to devise an effective qubit detector.

(Some figures in this article are in colour only in the electronic version)

## 1. Introduction

With the rapid advance in quantum information processing, quantum measurement (QM) in mesoscopic structures has attracted extensive attention in the last decade, both experimentally and theoretically [1–23]. To sum up, three kinds of QM detectors have been proposed so far: quantum point contact detectors, single quantum-dot (QD) detectors, and double quantum-dot (DQD) detectors. It has been demonstrated that quantum point contact can be utilized as an effective detector for reading out the quantum information stored in a charge-based DQD qubit [10–15]. Furthermore, it is suggested that the single QD structure is also useful for QM, which is more attractive than a quantum point contact detector in some aspects [16, 17]. Unfortunately, a single QD detector only can work at very low temperatures [9]. Recently, a new kind of detector, a DQD detector, has been found to be a sensitive detector which can perform well even at a relatively much higher temperature [18–23]. For the DQD detector scheme studied in [19–21], QM is implemented through the Coulomb interaction between electrons in QD-2 and QD-R (similar to figures 1(a) and (b), but the qubit is placed near QD-R). A comparison with the case in which the qubit is placed near QD-L demonstrates that putting the qubit near QD-L would lead to a worse performance [20]. One may wonder what happens if the qubit is placed near the potential barrier sandwiched between QD-L and QD-R. Is this geometrically *symmetrical* DQD detector still able to read out the qubit information effectively?

Now, we propose a novel QM scheme based on the positional rearrangement of the DQD detector and the qubit (see figure 1). In this new setup the qubit is placed right above the potential barrier between QD-L and QD-R, which makes the entire system, including the qubit and the detector, a completely symmetrical structure. As schematically shown in figure 1(c), the detector will work with a large-bias voltage, where the energy levels of two QDs are inside the chemical potentials $\mu_L$ of the left lead and $\mu_R$ of the right one, and the

 

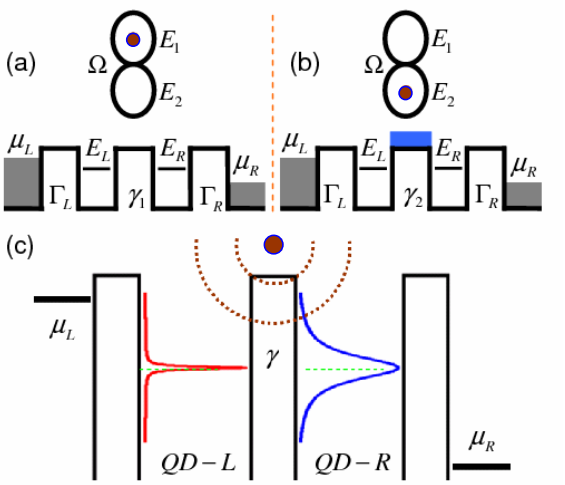


**Figure 1.** QM of the qubit (QD-1 and -2 coupled by interdot coupling Ω) through a detector, a coupled double QD (QD-L and -R), sandwiched between left and right leads. The electron evolving from QD-1 (a) to QD-2 (b) changes the detector interdot coupling from $\gamma_1$ to $\gamma_2$. (c) Energy diagram of a detector at work. The two curves in QD-L and -R show the density of states in the case of $\gamma = 0$. The filled circle above the barrier between two QDs denotes the electron in the qubit with the electrostatic potential represented by the dotted curves.

tunneling rates are much smaller than the chemical potential difference. In this case, the current is usually influenced by the energy level difference of QD-L and QD-R, as well as the interdot coupling. Obviously, the electrostatic potential induced by the electron in the qubit (denoted by a filled circle) will lead to the same effect on both the left and right halves separated by the barrier between QD-L and QD-R. Consequently the energy level difference of QD-L and QD-R is kept invariant in the process of qubit evolution. Therefore, the current variation is mainly or even *wholly* caused by the variation of the interdot coupling in the large-bias case. In principle, this kind of qubit–detector rearrangement is very interesting, for the following reasons: (i) *A longer dephasing time.* As is well known, in a symmetrical DQD structure an extra electron can tunnel back and forth between two QDs via the so-called Rabi oscillation. For most of time the electron dwells in two QDs and has little time to stay in the barrier region between two QDs. Very naturally, this short time for which the electron stays in the barrier region certainly reduces the duration of the qubit–detector interaction, thus increasing the dephasing time of the qubit. (ii) *A very large visibility.* If the interdot coupling $\gamma$ is devised to be relatively small, a moderate Coulomb interaction from the qubit electron can switch off the detector current, which enables one to obtain a convenient largest visibility of 2 (to be discussed below). (iii) *A very sensitive qubit–detector response region.* In this sensitive region, the same interdot coupling variation $\Delta\gamma = \gamma_1 - \gamma_2$, with $\gamma_1$ and $\gamma_2$ representing the interdot couplings in the detector when the qubit electron is localized in QD-1 and QD-2, respectively, will produce the largest current oscillation amplitude (i.e. the strongest signal), greatly beneficial to QM. Therefore, these adjustable physical parameters $\Gamma_R$, $\gamma$, and $\Delta\gamma$ can make one flexibly control and improve the quality of the QM. By precise parameter regulation, one can establish the optimal QM of the qubit information both with long dephasing time and strong signals.

With the aim of designing an effective DQD detector to perform a good QM of the dynamic qubit, we study quantum transport through the DQD detector first for a static qubit and then for a dynamic one. In the static qubit case, we find that there exists a sensitive qubit–detector response region as the detector current varies with the interdot coupling. Also, we find that the visibility of the current signal can be easily and greatly improved by adjusting the interdot coupling $\gamma$ and the difference $\Delta\gamma$. Then we turn to discuss QM of the dynamic qubit. It is demonstrated that the ratio $\Gamma_R/\gamma$ plays a crucial role in the quality of the QM while the interdot Coulomb interaction in the detector only leads to some quantitative modification of the detector current. Furthermore, we show that an increase in $\Gamma_R$ will make the dephasing time longer. Finally, we consider the effect of $\gamma_2$ and $\Delta\gamma$ on the quality of QM. It is demonstrated that for a certain $\Delta\gamma$, the signal amplitude can be enlarged by choosing a suitable $\gamma_2$ in the sensitive qubit–detector response region. However, for a certain $\gamma_2$, increase in $\Delta\gamma$ will make the qubit decay more quickly to a stationary state, suppressing the dephasing time.

The paper is organized as follows: In section 2 we derive the modified rate equation for the entire system. The transport properties of the DQD detector in the case of a static qubit are shown in section 3. Then we study the process of measuring the qubit information in section 4. Lastly a brief conclusion is outlined in section 5.

## 2. Modified rate equation

The entire setup shown in figure 1 can be modeled by the Hamiltonian $H = H_Q + H_D + H_I$ with

$$H_Q = E_1 a_1^\dagger a_1 + E_2 a_2^\dagger a_2 + \Omega(a_1^\dagger a_2 + \text{H.c.}), \tag{1a}$$

$$H_D = \sum_{\alpha=l,r,L,R} E_\alpha c_\alpha^\dagger c_\alpha + \gamma(c_L^\dagger c_R + c_R^\dagger c_L) + U n_L n_R + \left[\sum_l \Omega_l c_l^\dagger c_L + \sum_r \Omega_r c_r^\dagger c_R + \text{H.c.}\right], \tag{1b}$$

$$H_I = -\Delta\gamma a_2^\dagger a_2 (c_L^\dagger c_R + \text{H.c.}). \tag{1c}$$

Here $H_Q$, $H_D$, and $H_I$ denote the Hamiltonian of the qubit, the detector, and the interaction between them, respectively, while $a_{1,2}^\dagger(a_{1,2})$, $c_{L,R}^\dagger(c_{L,R})$, and $c_{l,r}^\dagger(c_{l,r})$ are the creation (annihilation) operators of the electron in the qubit, the two QDs in the detector, and the two leads. The parameters Ω and $\gamma$ represent the hopping amplitudes of the electron between the two single-QD states in the qubit and the detector, respectively, and $U$ denotes the Coulomb repulsion interaction between two electrons in two QDs of the detector. The detecting mechanism can be easily understood from a physical viewpoint. Obviously, the electron localized in QD-1 and QD-2 will induce a different variation of the electrostatic potential barrier between QD-L and QD-R. Certainly this variation will have some effect on the electrons flowing from the left lead through QD-L and QD-R to the right lead. It is expected that

one will be able to extract the quantum information stored in the qubit by detecting this response of the current to the charge distribution in the qubit. Mathematically, this is implemented by appending a qubit–detector interaction term, $H_{\rm I}$, which reflects that when the extra electron is in QD-2 an effective variation $\Delta\gamma$ appears and the resulting hopping amplitude becomes $\gamma_2 = \gamma_1 - \Delta\gamma$.

In order to find the current through the detector, one can use the basic current definition $I = {\rm d}Q/{\rm d}t$ to calculate the current through the $\alpha$th ($\alpha \in L$ or $R$) lead as $I_\alpha(t) = {\rm d}\langle eN_\alpha(t)\rangle/{\rm d}t$, where $N_\alpha(t)$ represents the number of electrons in lead-$\alpha$ at time $t$. Therefore, how to obtain this important physical parameter becomes a key step, which can be fulfilled by using the modified rate equations proposed by Gurvitz [24]. To begin with, let us first analyze the possible electron configurations in the reduced system with only four QDs. It can be found that there are four available states: ($a$), both QDs are empty; ($b$), only QD-L is occupied; ($c$), only QD-R is occupied; and ($d$), both QDs are occupied, with the extra qubit electron in QD-1. In the mean time, the corresponding states are denoted by ($a'$, $b'$, $c'$, $d'$) while the extra qubit electron stays in QD-2. According to the electron occupation in the right lead, the many-body wavefunction of the entire system can be written in the occupation number representation as

$$\begin{aligned}|\Psi(t)\rangle = &\left[V_a + \sum_l V_{{\rm b}l}c_{\rm L}^\dagger c_l + \sum_l V_{cl}c_{\rm R}^\dagger c_l\right.\\ &\left. + \sum_{l<l'} V_{dll'}c_{\rm L}^\dagger c_{\rm R}^\dagger c_l c_{l'} + \cdots\right]a_1^\dagger|0\rangle\\ &+\left[V_{a'} + \sum_l V_{b'l}c_{\rm L}^\dagger c_l + \sum_l V_{c'l}c_{\rm R}^\dagger c_l\right.\\ &\left. + \sum_{l<l'} V_{d'll'}c_{\rm L}^\dagger c_{\rm R}^\dagger c_l c_{l'} + \cdots\right]a_2^\dagger|0\rangle. \end{aligned} \tag{2}$$

Here, $|0\rangle$ is defined as a vacuum state with no electron in any QD and all the levels in both leads are initially filled with electrons up to the chemical potentials $\mu_{\rm L}$ and $\mu_{\rm R}$. All the $V_{\ldots}[\equiv V_{\ldots}(t)]$'s are the time-dependent probability amplitudes of finding the entire system in the corresponding states. For example, $V_{\rm bl}$ denotes the amplitude at which the qubit electron is localized in QD-1, and the electron initially in level $E_l$ is tunneled into QD-L with a hole being left in lead L. By substituting the Hamiltonian equation (1) and the wavefunction equation (2) into the time-dependent Schrödinger equation

$$i\hbar\frac{{\rm d}|\Psi(t)\rangle}{{\rm d}t} = H|\Psi(t)\rangle, \tag{3}$$

one can obtain an infinite set of linear algebraic equations for the probability amplitudes $V_{\ldots}$. Following Gurvitz's procedure we can derive the differential equations

$$\dot\rho_{aa}^n = -\Gamma_{\rm L}\rho_{aa}^n + \Gamma_{\rm R}\rho_{cc}^{n-1} + {\rm i}\Omega(\rho_{aa'}^n - \rho_{a'a}^n), \tag{4a}$$

$$\dot\rho_{a'a'}^n = -\Gamma_{\rm L}\rho_{a'a'}^n + \Gamma_{\rm R}\rho_{c'c'}^{n-1} + {\rm i}\Omega(\rho_{a'a}^n - \rho_{aa'}^n), \tag{4b}$$

$$\dot\rho_{bb}^n = \Gamma_{\rm L}\rho_{aa}^n + \Gamma_{\rm R}\rho_{dd}^{n-1} + {\rm i}\Omega(\rho_{bb'}^n - \rho_{b'b}^n) + {\rm i}\gamma_1(\rho_{bc}^n - \rho_{cb}^n), \tag{4c}$$

$$\dot\rho_{b'b'}^n = \Gamma_{\rm L}\rho_{a'a'}^n + \Gamma_{\rm R}\rho_{d'd'}^{n-1} + {\rm i}\Omega(\rho_{b'b}^n - \rho_{bb'}^n) + {\rm i}\gamma_2(\rho_{b'c'}^n - \rho_{c'b'}^n), \tag{4d}$$

$$\dot\rho_{cc}^n = -\Gamma_0\rho_{cc}^n + {\rm i}\Omega(\rho_{cc'}^n - \rho_{c'c}^n) + {\rm i}\gamma_1(\rho_{cb}^n - \rho_{bc}^n), \tag{4e}$$

$$\dot\rho_{c'c'}^n = -\Gamma_0\rho_{c'c'}^n + {\rm i}\Omega(\rho_{c'c}^n - \rho_{cc'}^n) + {\rm i}\gamma_2(\rho_{c'b'}^n - \rho_{b'c'}^n), \tag{4f}$$

$$\dot\rho_{dd}^n = \Gamma_{\rm L}'\rho_{cc}^n - \Gamma_{\rm R}\rho_{dd}^n + {\rm i}\Omega(\rho_{dd'}^n - \rho_{d'd}^n), \tag{4g}$$

$$\dot\rho_{d'd'}^n = \Gamma_{\rm L}'\rho_{c'c'}^n - \Gamma_{\rm R}\rho_{d'd'}^n + {\rm i}\Omega(\rho_{d'd}^n - \rho_{dd'}^n), \tag{4h}$$

$$\dot\rho_{aa'}^n = {\rm i}\Omega(\rho_{aa}^n - \rho_{a'a'}^n) - \Gamma_{\rm L}\rho_{aa'}^n + \Gamma_{\rm R}\rho_{cc'}^{n-1}, \tag{4i}$$

$$\dot\rho_{bb'}^n = {\rm i}\Omega(\rho_{bb}^n - \rho_{b'b'}^n) + {\rm i}\gamma_2\rho_{bc'}^n - {\rm i}\gamma_1\rho_{cb'}^n + \Gamma_{\rm L}\rho_{aa'}^n + \Gamma_{\rm R}\rho_{dd'}^{n-1}, \tag{4j}$$

$$\dot\rho_{cc'}^n = {\rm i}\Omega(\rho_{cc}^n - \rho_{c'c'}^n) + {\rm i}\gamma_2\rho_{cb'}^n - {\rm i}\gamma_1\rho_{bc'}^n - \Gamma_0\rho_{cc'}^n, \tag{4k}$$

$$\dot\rho_{dd'}^n = {\rm i}\Omega(\rho_{dd}^n - \rho_{d'd'}^n) + \Gamma_{\rm L}'\rho_{cc'}^n - \Gamma_{\rm R}\rho_{dd'}^n, \tag{4l}$$

$$\dot\rho_{bc}^n = {\rm i}\Omega(\rho_{bc'}^n - \rho_{b'c}^n) + {\rm i}\gamma_1(\rho_{bb}^n - \rho_{cc}^n) - \Gamma_0\rho_{bc}^n/2, \tag{4m}$$

$$\dot\rho_{b'c'}^n = {\rm i}\Omega(\rho_{b'c}^n - \rho_{bc'}^n) + {\rm i}\gamma_2(\rho_{b'b'}^n - \rho_{c'c'}^n) - \Gamma_0\rho_{b'c'}^n/2, \tag{4n}$$

$$\dot\rho_{bc'}^n = {\rm i}\Omega(\rho_{bc}^n - \rho_{b'c'}^n) + {\rm i}\gamma_2\rho_{bb'}^n - {\rm i}\gamma_1\rho_{cc'}^n - \Gamma_0\rho_{bc'}^n/2, \tag{4o}$$

$$\dot\rho_{b'c}^n = {\rm i}\Omega(\rho_{b'c'}^n - \rho_{bc}^n) + {\rm i}\gamma_1\rho_{b'b}^n - {\rm i}\gamma_2\rho_{c'c}^n - \Gamma_0\rho_{b'c}^n/2. \tag{4p}$$

Here, we assume $E_2 = E_1 = E_{\rm R} = E_{\rm L} = 0$ for those QDs in the qubit and detector, and define a new parameter $\Gamma_0 \equiv \Gamma_{\rm L}' + \Gamma_{\rm R}$ for convenience. The energy level bandwidths are defined as $\Gamma_{\rm L(R)} = 2\pi\rho_{\rm L(R)}(E_1)|V_{\rm L(R)}(E_1)|^2$ and $\Gamma_{\rm L}' = 2\pi\rho_{\rm L}(E_1)|V_{\rm L}(E_1+U)|^2$ with $\rho_{\rm L(R)}$ denoting the density of states in the left (right) lead. Finally, we can derive the currents through the right lead as

$$I_{\rm R}/e = \Gamma_{\rm R}(\rho_{cc} + \rho_{c'c'} + \rho_{dd} + \rho_{d'd'}). \tag{5}$$

## 3. Detector properties for a static qubit

Bear in mind that the objective of this paper is to extract the dynamic qubit information from the current flowing through the nearby DQD detector. However, the temporal and stationary detector currents are influenced by both the detector structure and the electron distribution in the qubit. That is to say, the detector structure will result in one kind of current variation by itself, which affects the qubit information readout. Therefore the important task is to obtain a global understanding of the current variations purely induced by the detector structure. No doubt this research will provide a criterion for distinguishing between what kind of current variation is induced by the detector and what is not.

First, we consider the stationary transport properties of the DQD detector. In the static qubit case ($\Omega = 0$), the extra electron in the qubit is localized in QD-1 or -2. Intuitively, the stationary current $\bar I_1$ (with the electron in QD-1) is larger than $\bar I_2$ (with the electron in QD-2), since the electron in QD-2 will give rise to a stronger suppression of the hopping amplitude $\gamma$. In these two peculiar cases, the original reduced eight-dimensional space splits into two subspaces $\{a, b, c, d\}$ and $\{a', b', c', d'\}$. Correspondingly, equation (4) will be classified into two groups: (i) equations (4*a*), (4*c*), (4*e*), (4*g*), (4*m*) and (ii) equations (4*b*), (4*d*), (4*f*), (4*h*), (4*n*). After solving them we can obtain the stationary current $\bar I_i/e = \gamma_i^2/(k\gamma_i^2 + k')$ where $k \equiv (\Gamma_{\rm R}^2 + 2\Gamma_{\rm L}\Gamma_{\rm R} + \Gamma_{\rm L}'\Gamma_{\rm L})/(\Gamma_{\rm L}\Gamma_{\rm R}\Gamma_0)$ and $k' \equiv \Gamma_0/4$. For convenience, we assume $\Gamma \equiv \Gamma_{\rm L} = 1$ as the energy unit. Therefore, the current can be rewritten using the dimensionless parameters $\tilde\gamma_i \equiv \gamma_i/\Gamma$, $\tilde\Gamma_{\rm R} \equiv \Gamma_{\rm R}/\Gamma$, and $\tilde\Gamma_{\rm L}' \equiv \Gamma_{\rm L}'/\Gamma$ as

$$\bar I_i = \frac{\tilde\gamma_i^2}{\tilde k\tilde\gamma_i^2 + \tilde k'}(\Gamma e), \tag{6}$$

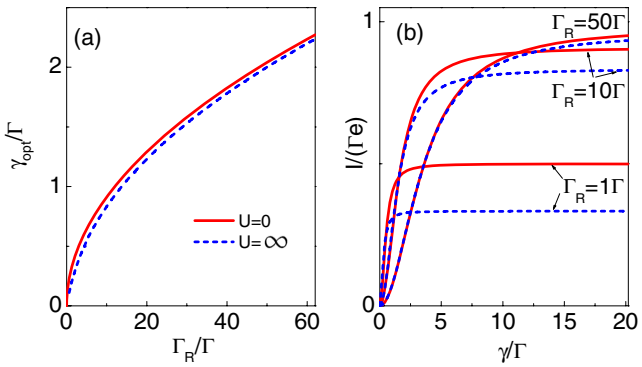


**Figure 2.** (a) Optimized interdot coupling $\gamma_{\rm opt}$ of the detector as a function of $\Gamma_{\rm R}$ in the case of $U = 0$ (solid curve) and $U = \infty$ (dashed curve). (b) The stationary currents flowing through the detector as a function of $\gamma$.

where $\tilde{k} \equiv (\tilde{\Gamma}_{\rm R}^2 + 2\tilde{\Gamma}_{\rm R} + \tilde{\Gamma}'_{\rm L})/(\tilde{\Gamma}_{\rm R}\tilde{\Gamma}_0)$ and $\tilde{k}' \equiv \tilde{\Gamma}_0/4$ with $\tilde{\Gamma}_0 \equiv \tilde{\Gamma}'_{\rm L} + \tilde{\Gamma}_{\rm R}$. We can easily find that $\bar{I}_i/(\Gamma e)$ increases monotonically with the increase of $\gamma_i$ for certain $\Gamma'_{\rm L}$ and $\Gamma_{\rm R}$, and eventually approaches the saturated value $1/\tilde{k}$ in the $\gamma_i \to \infty$ limit. By a simple analysis we may find a sensitive $\bar{I}_i \sim \gamma$ response region in the proximity of $\gamma_{\rm opt}/\Gamma \equiv \sqrt{k'/(3k)}$, where the largest current variation is able to be obtained for the same difference $\Delta\gamma$. For clarity we plot the optimized $\gamma_{\rm opt}$ as a function of $\Gamma_{\rm R}$ in both cases: $U = 0$ and $U = \infty$ (see figure 2(a)). It can be found that with increasing $\Gamma_{\rm R}$, $\gamma_{\rm opt}$ is increased in both cases. The most conspicuous difference is that the optimized interdot coupling for $U = 0$ is slightly larger than that of $U = \infty$, which only makes a quantitative difference. This also implies that $U$ only plays a trivial role.

Furthermore, we select some sample points ($\tilde{\Gamma}_{\rm R} = 1$, 10, and 50) to explore the effects of $\gamma$ on the detector currents, which are shown in figure 2(b). Let us observe the solid curves ($U = 0$) first. We can find a steep slope in every $I$–$\gamma$ curve before the current saturates. This steep slope is the most sensitive qubit–detector response region, which is beneficial for designing a sensitive detector. This slope is still observed in the case of $U = \infty$ (see the dotted curves in figure 2(b)), further demonstrating that $U$ only plays a quantitative role.

In figure 3 we consider another important parameter, the visibility, to characterize the detector; this is defined as $P \equiv 2|I_1 - I_2|/(I_1 + I_2)$ [12]. We can see that the visibility is increased with an increase in $\Delta\gamma$ but a decrease in $\gamma_2$. By comparing those two images in figure 3 we can find that the visibility is increased with $\Gamma_{\rm R}$. In order to design a sensitive detector with higher $P$, we would better carefully optimize the detector and qubit parameters by taking into account the following factors: (i) a relatively larger $\Gamma_{\rm R}$ and $\Delta\gamma$ and (ii) a weaker $\gamma_2$. This may be viewed as a reference for designing a DQD detector. It should be pointed out that with this DQD detector scheme it is easier to obtain the largest visibility of $P = 2$ just by assuming $\gamma_2 = 0$ (i.e. $I_2 = 0$).

## 4. Measuring dynamic qubits

In this section, we study how to measure the dynamic information stored in qubit. For simplicity we assume $\hbar = 1$, $e = 1$, and the interdot coupling $\Omega$ in the qubit is always $1\Gamma$. The initial condition for QM corresponds to the case in which the qubit electron is localized in QD-1 and the detector current $I = \bar{I}_1$. This requires that the detector first evolves into its stationary state, and then the qubit operation is switched on. Based on the discussion in section 3 we assume $\gamma_1 = \Gamma$ and $\gamma_2 = 0$ to ensure QM is carried out with the largest visibility of $P = 2$.

Figure 4 shows the time-dependent evolution of the probability $\rho_{11}$ (solid curves) and the current $I(t)$ (dotted curves) for the symmetric ($\Gamma_{\rm R} = \Gamma_{\rm L}$) and asymmetric ($\Gamma_{\rm R} \neq \Gamma_{\rm L}$) detectors. First, we inspect those curves in figures 4(a)–(c) with $U = 0$ for different $\Gamma_{\rm R}$. Both the current $I(t)$ and the corresponding probability $\rho_{11}$ display oscillations as a function of time. For the small $\Gamma_{\rm R} = 1\Gamma$ (see figure 4(a)), the detector cannot follow the qubit oscillations very well. However, when $\Gamma_{\rm R}$ is tuned sufficiently large (e.g. $\Gamma_{\rm R} = 50\Gamma$), the detector is inclined to keep up with the qubit oscillation, which enables us to extrapolate the qubit information from the current oscillations, in agreement with the results obtained by Gilad and Gurvitz [19]. This can be well understood as follows: when $\Gamma_{\rm R}$ is much greater than $\gamma_1$, the electron in QD-2 will spend a much shorter time entering the right lead than returning to QD-L. Obviously, on the one hand this will decrease the probability of the electron in QD-2 going back to QD-L, suppressing the multiple interaction between the qubit and the detector; on the other hand the electron is

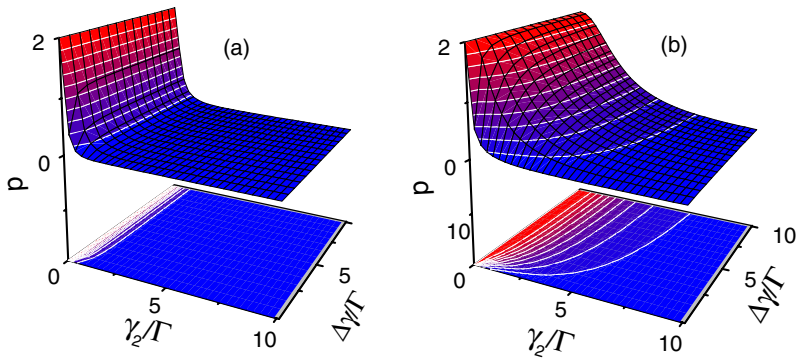


**Figure 3.** Stationary current visibility $P$ as a function of $\gamma_2$ and $\Delta\gamma$ in the case of (a) $\Gamma_{\rm R} = 1\Gamma$ and (b) $\Gamma_{\rm R} = 50\Gamma$.

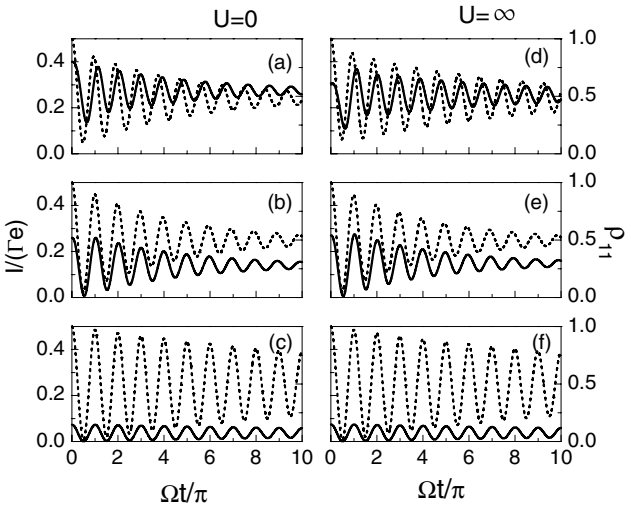


**Figure 4.** Time-dependent evolution of the current (solid curve) and the corresponding electron probability $\rho_{11}$ (dotted curve). In the case of $U = 0$ ($U = \infty$), (a), (b), and (c) ((d), (e), and (f)) correspond to $\Gamma_R/\Gamma = 1$, 10, and 50, respectively.

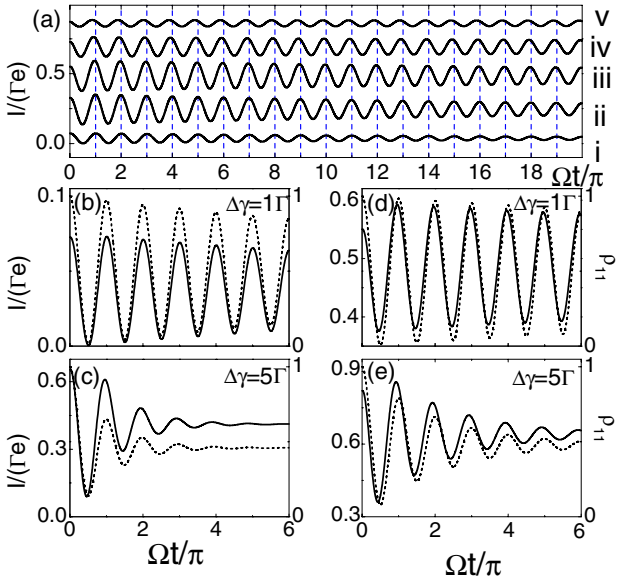


**Figure 5.** (a) Time-dependent currents with $\Gamma_R = 50\Gamma$ and $\Delta\gamma = 1\Gamma$ for different interdot couplings $\gamma_2/\Gamma =$ (i) 0, (ii) 1.5, (iii) 3, (iv) 5, and (v) 9. Parts ((b), (c)) and ((d), (e)) display the time-dependent current (solid curve) and corresponding probability $\rho_{11}$ (dotted curve) for $\gamma_2/\Gamma = 0$ and 3, respectively.

quickly transmitted into the right lead, reducing the dwell time of the electron in QD-R and avoiding the destruction of any electron-carried qubit information. Consequently, the electron distribution in the qubit can be effectively reproduced by the current signal. Reduction of the interaction time between the detector and the qubit can also be observed from the decay behavior of the probability $\rho_{11}$, as shown by the dotted curves in figures 4(a)–(c). As $\Gamma_R$ increases the decay becomes slower, reflecting the reduction of the interaction time. However, one can find that the current oscillation amplitudes become smaller, as already shown in figure 2(b), which requires a more sensitive external current meter for measurement. Then we study the effect induced by the Coulomb interaction $U(=\infty)$ in figures 4(d)–(f). It is clear that in the case of $\Gamma_R = 1\Gamma$ (figure 4(d)) the Coulomb interaction will induce sharp differences in the current curve in comparison with the case of $U = 0$ (figure 4(a)). As $\Gamma$ increases, the difference becomes negligibly small. This demonstrates that $U$ only make quantitative modifications to the currents and probabilities, indicating that it only plays a trivial role in the detection process.

Then we explore the effect of $\gamma$ in figure 5(a) when $\Delta\gamma = 1\Gamma$. In the case of $\gamma_2 = 0$ and $\gamma_2 = 9\Gamma$ (far away from $\gamma_{opt} \approx 2\Gamma$) the oscillation amplitude is very small, while it is large in the proximity of $\gamma_2 = 1.5\Gamma$ and $\gamma_2 = 3\Gamma$, as expected from figure 2. This verifies that a proper selection of $\gamma_2$ will give a larger oscillation amplitude, which is beneficial to QM. However, one may ask whether the increase in $\gamma_2$ will destroy the quality of the detection, since a condition for good QM is $\Gamma_R/\gamma \gg 1$. In principle, the electron oscillation period in a qubit should be $\pi$, since the interdot coupling is 1. Nevertheless, the period becomes shorter than $\pi$ when $\gamma_2$ is large enough (e.g. $\gamma_2 = 9\Gamma$). This implies that the increase in $\gamma_2$ will affect the quality of the QM. Furthermore, by a statistical analysis of the positions of the peaks and troughs in the $\rho_{11}$ curves, we find that $\gamma_2$ leads to only tiny variations of these positions if $\gamma_2$ is kept sufficiently weak in contrast to $\Gamma_R$ (which are not listed here). Also, we find that the mismatch between most of the peaks in the $\rho_{11}$ curve and the corresponding peaks in the current is negative when $\gamma_2 = 0$ and becomes positive when $\gamma_2$ is enough large (e.g. $\gamma_2 = 1.5$), indicating that there should be a transition position where the mismatch is almost zero.

Finally, let us pay attention to the influence of $\Delta\gamma$. Figures 5(b)–(e) show the evolution curves for both the weak measurement regime $\Delta\gamma = 1\Gamma$ and the strong one $\Delta\gamma = 5\Gamma$ in two cases: $\gamma_2 = 0$ ((b), (c)) and $\gamma_2 = 3\Gamma$ ((d), (e)). Through a global comparison two distinct characteristics can be found: (i) An increase in $\Delta\gamma$ will lead to a much larger oscillation amplitude, which can be found from the curves in the initial stage. For example, in figure 5(c) the initial current oscillation amplitudes ($\gg 0.1\Gamma e$) for $\Delta\gamma = 5\Gamma$ are obviously much larger than those ($<0.1\Gamma e$) of $\Delta\gamma = 1\Gamma$ (see figure 5(b)). This is also the case in figures 5(d) and (e). (ii) Another important characteristic is that the decay of the current and probability oscillations becomes quicker as $\Delta\gamma$ increases. This demonstrates that although this $\Delta\gamma$ increase produces a stronger amplitude which is beneficial for QM, it also induces a quicker decay in the current signal, shortening the dephasing time. This result indicates that a suitable $\Delta\gamma$ should be designed in order to keep a sufficiently strong signal to measure and a long enough decay time to perform quantum operations.

## 5. Conclusion

In conclusion, a novel type of DQD detector is utilized to detect the dynamic qubit information. By inspecting the stationary

detector current for the static qubit, we find a sensitive qubit–detector response region, indicating that a suitably chosen interdot coupling can produce a larger detector current signal. Furthermore, we show that a good QM of a qubit is inclined to be established by increasing the right dot–lead coupling. Nevertheless, the interdot Coulomb interaction has only a trivial role in the quality of the QM. Moreover, we study the dephasing of the qubit induced by the detector.

## Acknowledgments

This work is financially supported by the NSFC under grant nos 10547105 and 10604005, and the Excellent Young Scholars Research Fund of Beijing Institute of Technology (no. 2006Y0713).

## References

[1] Buks E, Schuster R, Heiblum M, Mahalu D and Umansky V 1998 *Nature* **391** 871
[2] Schoelkopf R J, Wahlgren P, Kozhevnikov A A, Delsing P and Prober D E 1998 *Science* **280** 1238
[3] Macucci M, Gattobigio M and Iannaccone M 2001 *J. Appl. Phys.* **90** 6428
[4] Elzerman J M, Hanson R, Willems van Beveren L H, Witkamp B, Vandersypen L M K and Kouwenhoven L P 2004 *Nature* **430** 431
[5] Xiao M, Martin I, Yablonovitch I and Jiang H W 2004 *Nature* **430** 435
[6] Gustavsson S, Leturcq R, Simovic B, Schleser R, Studerus P, Ihn T, Ensslin K, Driscoll D C and Gossard A C 2006 *Phys. Rev.* B **74** 195305
[7] Fujisawa T, Hayashi T, Tomita R and Hirayama Y 2006 *Science* **312** 1634
[8] Onac E, Balestro F, Willems van Beveren L H, Hartmann U, Nazarov Y V and Kouwenhoven L P 2006 *Phys. Rev. Lett.* **96** 176601
[9] Devoret M H and Schoelkopf R J 2000 *Nature* **406** 1039
[10] Gurvitz S A 1997 *Phys. Rev.* B **56** 15215
[11] Korotkov A N 1999 *Phys. Rev.* B **60** 5737
[12] Li X Q, Zhang W K, Cui P, Shao J S, Ma Z S and Yan Y J 2004 *Phys. Rev.* B **69** 085315
[13] Korotkov A N and Jordan A N 2006 *Phys. Rev. Lett.* **97** 166805
[14] Goan H-S, Milburn G J, Wiseman H M and Bi S H 2001 *Phys. Rev.* B **63** 125326
[15] Tanamoto T and Hu X 2005 *J. Phys.: Condens. Matter* **17** 6895
[16] Shnirman A and Schön G 1998 *Phys. Rev.* B **57** 15400
[17] Gurvitz S A and Berman G P 2005 *Phys. Rev.* B **72** 073303
[18] Tanamoto T and Hu X 2004 *Phy. Rev.* B **69** 115301
[19] Gilad T and Gurvitz S A 2006 *Phys. Rev. Lett.* **97** 116806
[20] Geszti T and Bernád J Z 2006 *Phys. Rev.* B **73** 235343
[21] Jiao H J, Li X Q and Luo J Y 2007 *Phys. Rev.* B **75** 15533
[22] Brenner R, Greentree A D and Hamilton A R 2003 *Appl. Phys. Lett.* **83** 4640
[23] Brenner R, Buehler T M and Reilly D J 2005 *J. Appl. Phys.* **97** 034501
[24] Gurvitz S A and Prager Y S 1996 *Phys. Rev.* B **53** 15932